1

2

A grey box model of glucose fermentation and

3

syntrophic oxidation in Microbial Fuel Cells

4   **Maria de los Ángeles Fernandez[1,2], Maria de los Ángeles Sanromán[2], Stanislaw**

5   **Marks[1,3], Jacek Makinia[3], Araceli Gonzalez del Campo[1], Manuel Rodrigo[1], Francisco**

6   **Jesus Fernandez[*1]**

7   [1]University of Castilla-La Mancha, ITQUIMA, Chemical Engineering Department,

8   Avenida Camilo José Cela S/N. 13071 Ciudad Real, Spain.

9   [2]University of Vigo, Department of Chemical Engineering, Isaac Newton, Vigo, Spain

10   Building, Campus As Lagoas, Marcosende 36310 Vigo, Spain

11   [3]Gdansk University of Technology, Faculty of Civil and Environmental Engineering,

12   Gabriela Narutowicza 11/12, 80-233 Gdansk, Poland.

13

14

15

16

17

18   * Corresponding author: Francisco Jesús Fernández Morales

19   University of Castilla-La Mancha, ITQUIMA, Chemical Engineering Dept., Avda. Camilo

20   José Cela S/N 13071, Ciudad Real, Spain.

21   Tel: 0034 926 295300 (ext. 6350), Fax: 0034 926 295242.

22   E-mail: FcoJesus.FMorales@uclm.es

23

24   **Abstract**

25   In this work, the fermentative and oxidative processes taking place in a microbial fuel

26   cell (MFC) fed with glucose were studied and modeled. The model accounting for the

27   bioelectrochemical processes was based on ordinary, Monod-type differential

28   equations. The model parameters were estimated using experimental results obtained

29   from three H-type MFCs operated at open or closed circuits and fed with glucose or

30   ethanol. The experimental results demonstrate that similar fermentation processes

31   were carried out under open and closed circuit operation, with the most important

32   fermentation products being ethanol (with a yield of 1.81 mol mol^{-1} glucose) and lactic

33   acid (with a yield of 1.36 mol mol^{-1} glucose). A peak in the electricity generation was

34   obtained when glucose and fermentation products coexisted in the liquid bulk.

35   However, almost 90% of the electricity produced came from the oxidation of ethanol.

36

37

39

1. Introduction

Due to increasing energy demands and environmental concerns, the interest in the development of renewable energy sources as alternatives to fossil fuels has increased in recent years (MacKie et al., 2013). At the same time, more stringent environmental requirements for wastewater treatment are pressing for the development of more efficient treatment techniques. This phenomenon is not only an environmental concern but also an economical issue because water and wastewater systems are significant energy consumers. For example, an estimated 3-4% of U.S. electricity is consumed by the water and wastewater industry (Chandrappa & Das, 2014). In such a scenario, a reduction in treatment costs is necessary. Currently, the most important operational cost in a conventional wastewater treatment plant (WWTP) is aeration (Fernández et al., 2011a). Thus, the development of a process allowing for the oxidation of the pollutants with lower aeration requirements is of crucial importance.

Currently, the most adequate technology for solving the combined energetic and environmental problem seems to be bioelectrochemical technology. Because of that, bioelectrochemical systems, including Microbial Fuel Cells (MFCs) and Microbial Electrolysis Cells (MECs), have been investigated as alternative energy sources and wastewater treatment systems (Brillas & Martínez-Huitle, 2015).

MFCs are electrochemical devices that can directly convert organic and inorganic substrates into electricity by means of a microbial culture. MFCs mimic a biological system, with the only difference being that they do not transfer electrons directly to the electron acceptor. Instead, the MFC anodofilic bacteria transfer the electron to a solid electrode as part of their respiration pathway. Then, the electron is externally conducted over the anode to the cathode, which results in the production of electricity

3

64 (Rao et al., 1976). Because of this ability, the interest in MFC is increasing due to its

65 dual benefit: the production of green electricity and the oxidation of wastewater

66 components without an oxygen supply (Picioreanu et al., 2008). The main advantages

67 of these devices are the mild operational conditions (neutral pH and ambient

68 temperature) and the unlimited range of potential fuels that could be used (Schröder,

69 2007), including wastes and fuels for which catalysts are currently unavailable.

70 In the MFC, one of the most widely used fuels is glucose. Glucose has been proposed

71 as an interesting renewable energy source because it is safe (non-flammable and non-

72 toxic) and its energy density (16 Mj Kg^{-1}) is lower than that of methanol or gasoline but

73 is still quite high. Moreover, glucose is a basic unit of organic compounds that

74 abundantly exist in wastewater. Therefore, glucose seems to be a powerful and

75 environmentally friendly option.

76 Glucose-rich wastewaters can be found in different industries, but the industry

77 producing the highest amounts is the agro-food industry (De Lucas et al., 2005). Agro-

78 food wastewaters are characterized by very high organic loads and biodegradability

79 (Rodríguez et al., 2007). The development of a technology capable of efficiently using

80 the glucose contained in agro-food wastewater is of crucial importance to developing

81 real applications of the MFC technologies.

82 The main drawback of the use of glucose as a fuel in the MFC is that glucose-rich

83 streams give rise to only a small current when they are used as fuel in the MFC (Kim et

84 al., 2007; Lee et al., 2008). This small current occurs because glucose is a complex

85 substrate, and glucose can be used as a substrate in a large number of non-

86 electrogenic anaerobic processes (Freguia et al., 2008).

87 During the operation of MFCs, multiple/parallel bioelectrochemical reactions take

88 place. One of these simultaneous processes is fermentation. Fermentation and

89 electrogenesis are two primary steps in bioelectrochemical systems (Premier et al.,

90 2013). The objective of fermentation is to transform organic materials into the end

91 products of liquids and gases through a variety of bioconversion stages (Fernández et

92 al., 2011b). Several MFC studies have shown that fermentation and anode respiration

93 processes are often combined (Freguia et al., 2008). Fermentative bacteria are able to

94 ferment complex organic substrates to short-chain fatty acids (SCFA), alcohols and

95 other fermentation products. All of these products can subsequently be oxidized to

96 produce electricity (Kim et al., 2007). Integrating both processes in the anodic chamber

97 may have a positive influence on the overall efficiency of wastewater treatment and

98 the generation of electricity. Therefore, the description of the fermentation process at

99 the anodic chamber of MFCs is of great interest.

100 One of the most economical and appropriate approaches to investigating the microbial

101 behavior of and to comprehending the bioelectrochemical interactions in both MFCs

102 and MECs is through mathematical modeling (Karimi Alavijeh et al., 2015). Modeling

103 efforts have also been directed towards several aspects related to MFCs, evolving in

104 recent years from simple to complex models, such as multi-species, multi-dimensional

105 or multiscale models (Ortiz-Martínez et al., 2015). In the literature, there are papers

106 discussing generalized models describing wastewater treatment and the associated

107 energy production on MFC (Karimi Alavijeh et al., 2015), models of MFC biofilms and

108 suspended cultures (Picioreanu et al., 2010a), models of inorganic pollutants and pH

109 effects on MFC (Picioreanu et al., 2010b) and papers reviewing and classifying the

110 existing models (Ortiz-Martínez et al., 2015).

111   In this context, the objective of this study was to evaluate the performance of a MFC

112   fed with glucose in order to study the influence of the fermentation process and the

113   syntrophic oxidation of the fermentation products generated on the performance of

114   the MFC.

115

116

2. Materials and methods

2.1 MFC Model definition

119 To clarify the glucose transformations in the MFC, the fermentation process and the

120 subsequent oxidation of the fermentation products were modelled. The model

121 definition was based on experimental observations when studying the fermentative

122 and subsequent oxidative processes in the H-type MFCs used in this work. These

123 equations are presented in the form of the Petersen matrix in Table 1, and the

124 parameters of the model are presented in Table 2. All of the kinetics expressions are

125 based on the classical, commonly-used Monod terms (Monod, 1949). The equations

126 address the soluble compounds involved anaerobic and electrogenic transformations.

127 Thus, the effect of the concentration of the mediator in oxidized form was included in

128 the electrogenic processes (Picioreanu et al., 2010a).

129 [TABLE 1 NEAR HERE]

130 [TABLE 2 NEAR HERE]

131 In the developed model, the reactions proposed included glucose fermentation to

132 fermentation products (via non-electrogenic fermentation processes) and the

133 oxidation of glucose and the fermentation products to produce electricity. The

134 fermentation was considered to be non-electrogenic because the main fermentation

135 products accumulated in the liquid bulk of both MFCs (open and closed circuit)

136 correspond to those not generated by means of the electricity generation processes.

137 On the other hand, based on the experimental results, the main electrogenic reactions

138 were the electrogenic oxidation of glucose and the main fermentation product (i.e.,

139 ethanol) to CO_2.

140   When the anodic and cathodic chambers were connected via the external electrical

141   circuit (i.e., closed circuit), the environmental conditions required for electrogenic

142   metabolism by the organisms were obtained. In contrast, the fermentative processes,

143   rather than the electrogenic ones, may be the predominant processes when working

144   under open circuit conditions. Through the comparison of MFCs of both circuit types

145   (closed and open), the fermentation and electrogenic metabolisms were

146   discriminated.

147   Taking into account the similarities observed when working with the open and closed

148   circuit MFCs, the fermentation equations proposed for the open circuit MFC were also

149   used for the closed circuit MFC. The only difference was the existence of a lag phase

150   when fermenting glucose to lactic acid under closed circuit conditions but not under

151   open circuit conditions. To describe both behaviors, a switching function in the lactic

152   acid production rate was included (see process B2 in Table 2). The different behavior of

153   the closed circuit MFC could be explained because of the ability of the microorganisms

154   to switch between glucose oxidation with electricity production and lactic acid

155   generation from glucose fermentation. The switching function was based on an

156   inhibition function proposed in the literature (Edwards, 1970). In this function, an

157   additional term called I_x was included. This term is a Boolean function with a value of 0

158   for open circuit and 1 for closed circuit. The inclusion of this term allowed us to

159   describe the differences in the fermentation under open or closed circuit conditions.

160   Additionally, the glucose and fermentation products generated could be oxidized to

161   carbon dioxide, thereby generating electricity. The equations describing these

162   processes in the model are processes E1 and E2 (Table 2). A reaction-scheme of the

163   proposed model is depicted in Figure 1.

8

164   FIGURE 1 NEAR HERE

165   Neither hydrogen production by fermenters nor methane production by methanogens

166   were included in the developed model because neither methane nor hydrogen were

167   detected in the gas phase of the H-type MFC. The lack of methane in the gas phase

168   could be explained because of the acidification of the anodic chamber, which inhibits

169   the activity of the methanogenic microorganisms (Fernández-Morales et al., 2010).

170   Regarding hydrogen, its absence could be related to the seed used for the inoculation

171   of the MFC. Acetic and formic acids only appeared in trace concentrations, in both

172   open and closed circuit experiments, and therefore they were not included in the

173   model.

174   Taking into account the processes identified, the calibration was performed in three

175   stages. In the first stage, the calibration was focused on the non-electrogenic

176   fermentation processes. In the second stage the electrogenic ethanol oxidation was

177   modeled. Finally, a third stage was used to simultaneously study the whole system,

178   including the glucose fermentation and the electrogenic glucose and ethanol

179   consumption, as well as the associated electricity generation.

180   To determine the best fit of the model, mathematical calculations were performed

181   using the Solver Tool in MS Excel. These calculations required the calculation of the

182   minimum residual sum of squared errors, which is associated with the difference

183   between the experimental data and the theoretical predictions of the model (de Lucas

184   et al., 2007).

185

186   *2.2 MFC Design and configuration*

187   Dual-compartment H-type MFCs were used. The MFCs held 0.7 L in each compartment,

188   and the compartments were separated by a tubular central compartment into which

189   the separator was located (see Figure 2). The separator used in this work was a 5 cm

190   thick microporous separator, including 16 cm^3 of compacted kaolin powder (with

191   particle diameters less than 35 microns). This separator was supported by a glass fiber

192   filter to avoid disintegration due to the action of bulk liquid at both anodic and

193   cathodic sides of the separator. The separator was designed to avoid the transport of

194   microorganisms from the anodic to the cathodic chamber and to avoid the transport of

195   oxygen from the cathodic to the anodic chamber. It must be stated that the MFC used

196   in this work was mainly limited due to the internal resistance of the separator;

197   therefore, the results are not directly applicable to a single-chamber MFC. The

198   electrodes used in both the anode and the cathode were porous graphite rods (1 cm

199   OD x 10 cm L) without any surface treatment or catalytic addition. Before the

200   experiments, the electrodes were first soaked in deionized water for a period of 24 h.

201   The submersible external surface of each electrode was 25.9 cm^2. The electrodes were

202   placed at a distance of 20 cm on either side of the MFC. Cooper wires and a 120 ohm

203   resistor were used as a contact from the electrodes. The cathode was continuously

204   aerated by using an aquarium air pump. During the experiments, the air pump

205   supplied 6 L min^{-1} of air at 1.5 atmospheres of pressure to the cathodic chamber.

206   Three identical H-type MFCs were used to study different processes, including

207   electricity production from glucose, electricity production from the main fermentation

208   product (ethanol), and the glucose fermentation process. In the latter case, the

209   fermentation process was isolated from the electricity production process by

210   disconnecting the external electrical circuit.

211   [FIGURE 2 NEAR HERE]

212

213 *2.3 MFC operation*

214 The anodic chamber of the MFCs were fed with a medium solution containing the

215 organic substrate, 9 g L of glucose or 3.3 g L of ethanol (depending on the test) and the

216 following trace minerals (in g L^{-1}): NH_4Cl 3.0150; KH_2PO_4 1.7550; NaCl 0.6570; Na_2SO_4

217 0.1290; $MgCl_2$ $6H_2O$ 0.2700; EDTA 0.1125; $ZnSO_4$ $7H_2O$ 0.0072; $FeSO_4$ $7H_2O$ 0.0070;

218 $MnCl_2$ $4H_2O$ 0.0056; CuCl $2H_2O$ 0.0050; $CoCl_2$ $6H_2O$ 0.0022; $CaCl_2$ 0.0014; $NiCl_2$ $6H_2O$

219 0.0011; Na_2MoO_4 $2H_2O$ $0.225 \cdot 10^{-3}$; and H_3BO_4 $0.225 \cdot 10^{-3}$. The carbon and mineral

220 solution was sterilized in an autoclave at 110 °C for 20 min. A high organic substrate

221 concentration was used to identify non-electrogenic anaerobic reactions and also to

222 maintain a longer energy production in the batch microbial fuel cell. The cathodic

223 chamber was fed with demineralized water.

224 The anodic chambers of the MFCs were seeded two days after the start-up of the

225 MFCs with a selectively enriched mixed culture taken from the effluent of a working

226 MFC (Gonzalez del Campo et al., 2013). By working in this way, the absence of

227 electricity generation before the seed of the MFC was verified, serving these data as

228 abiotic control data.

229 All of the experiments were conducted in batch mode. The experiments were

230 continued until there was no significant change in the measured quantities. The

231 contents in the anode and cathode chambers were continuously homogenized by

232 means of magnetic stir bars rotating at 80 rpm. The power output was monitored by

233 measuring voltage with an external resistor (120 ohms) connected between the

234 electrodes.

235

236 *2.4 Analytical methods and calculations*

237 Aqueous samples were collected from each MFC and then immediately centrifuged

238 (12000 rpm) and filtered through a 0.45 µm membrane filter. Once filtered, the

239 samples were analyzed or preserved frozen, according to the procedures described in

240 the literature (Eaton et al., 2005).

241 Glucose concentrations were measured by HPLC (Agilent) with a refractive index

242 detector (series 1200). A Zorbax Carbohydrate Column (4.6 x 150 mm, 5-micron) was

243 used to separate the components at 35 °C using a mobile phase composed of 75%

244 acetonitrile and 25% water v/v and a flow rate of 1.5 cm^3 min^{-1}. Furthermore, lactic

245 acid was determined from centrifuged and filtered samples by HPLC (Agilent) equipped

246 with UV-DAD and Zorbax SB-Aq (4.6 x 150 mm, 5-micron). The mobile phase was a

247 buffer at pH 2 (0.05 M phosphate). SCFA (acetic, propionic and butyric) and ethanol

248 contents were determined from a centrifuged (12000 rpm) and filtered sample (0.45

249 µm membrane) by gas chromatography (Perkin Elmer) with a flame ionization detector

250 (FID) using a Crossbond Carbowax Column (15 m x 0.32 mm ID, 0.25 mm df). The initial

251 temperature of the oven was 140 °C, which held for for 1.5 min, and the temperature

252 was raised at 25 °C min^{-1} until 190 °C, where it was maintained for 2 min. The

253 temperature of the injector and detector were 200 °C and 230 °C, respectively.

254 Nitrogen was used as the carrier gas. More information can be found elsewhere

255 (Fernández-Morales et al., 2010; Infantes et al., 2011). pH values were determined

256 using a Crison GLP-22 pH probe (Crison Instruments S.A., Barcelona, Spain).

257 Bioelectrochemical calculations were carried out based on the procedures outlined in

258 the literature (Logan et al., 2006). Potential (V) measurements were recorded with an

259 auto range digital multimeter (Model 2700, Keithley Instrument, OH, USA). Coulombic

12

260 efficiency (CE), defined as the ratio of the total coulombs actually transferred to the

261 anode from the substrate to the maximum possible coulombs if all substrate removal

262 produces the electrical current (Logan et al., 2006), was calculated by integrating the

263 current over time and taking into account the total Coulombs associated with the COD

264 removed in the same period of time.

265

266
$$CE = \frac{M \int_0^t I \, dt}{F \, b \, V \, \Delta COD}$$

267

268 where M is the molecular weight of oxygen (32), I corresponds to the current intensity

269 generated, F is Faraday's constant (96.485 C mol^{-1} e^{-}), b represents the number of

270 electrons exchanged per mole of COD removed (4), V is the volume of liquid in the

271 anode compartment (0.7 L), and ΔCOD depicts the change in theoretical COD

272 concentration over the period of time. The COD concentrations were theoretically

273 calculated based on the substrate concentration in the bulk liquid. In this way, it is

274 possible to isolate the contribution of each product in every process. To ratify the

275 accuracy of the theoretical COD calculations, the actual COD concentration of each

276 sample was experimentally determined and compared with the theoretical

277 concentration, with the error in all cases being lower than 8%. The gas composition

278 was analyzed by a multi-component gas analyzer (Rosemount Analytical NGA 2000

279 MLT, Emerson).

280

3. Results and Discussion

281

282 Before the study and modeling of the results, the mass balance in all the experiments

283 performed was verified. Table 3 presents the carbon balance in the glucose-fed MFC

284 (open and closed circuit) and the ethanol-fed MFC. As seen from Table 3, the carbon

285 recovery was approximately 90%.

286 [TABLE 3 NEAR HERE]

287

288 3.1 Open circuit MFC

289 To isolate and to study the fermentative processes taking place in the H-type MFC, an

290 open circuit experiment was performed. Working in this way, the glucose was

291 fermented but not oxidized by electroactive microorganisms. During the operation, the

292 liquid bulk of the anodic chamber was analyzed, and the concentrations of the main

293 compounds were determined. The experimental results obtained are presented in

294 Figure 3.

295 [FIGURE 3 NEAR HERE]

296 It can be seen in Figure 3 that glucose was fully consumed after approximately 15 d.

297 Regarding the glucose consumption, it must be noted that a reduction in pH was

298 observed from neutrality to pH values near 5.5, which indicates the existence of the

299 fermentation process. Several fermentation products appeared as a result of the

300 fermentation process. The main fermentation products were ethanol and lactic acid,

301 accounting for more than 95% of the fermentation products generated. In addition,

302 acetic and formic acids appeared in trace concentrations (data not shown). The

14

303   maximum concentrations of ethanol and lactic acids reached approximately 6.7 and

304   3.4 g COD L^{-1}, respectively.

305   With the aim of using this information for the description of the processes taking place

306   in the closed circuit H-type MFC, the model equations corresponding to the glucose

307   fermentation processes were fitted to the experimental data. From the fitting, the

308   main kinetics and stoichiometric parameters were determined. The yields of the main

309   fermentation products, ethanol and lactic acid, were 0.88 and 0.68 g COD per g COD of

310   glucose consumed, respectively, and the maximum specific uptake rates were 2.3 g

311   COD (g COD d)$^{-1}$ and 1.2 g COD (g COD d)$^{-1}$ for ethanol and lactic acid, respectively. The

312   glucose half-saturation coefficient (K_s) was 1.93 g COD L^{-1} in both cases. As seen in

313   Figure 3, the model accurately predicts the substrate and product concentrations along

314   the fermentation experiment.

315   The equations proposed and the parameter values obtained were subsequently used

316   to fit the closed circuit experimental data set obtained when glucose was used for the

317   electricity generation.

318

319   3.2 Closed circuit MFC

320   With the aim to studying the fermentative and electrogenic processes simultaneously

321   occurring in the H-type MFC, a closed circuit experiment with glucose and feedstock

322   was performed. During the experiment, the patterns of change of the main variables

323   were determined.

324   *3.2.1 Power generation and theoretical COD removal*

325   Before the inoculation, the anodic chamber of the H-type MFC was operated with the

326   sterilized wastewater in the absence of biocatalyst for a period of 2 d. During this

15

327 period, the electricity generation was negligible. Subsequently, the H-type MFC was

328 seeded. The H-type MFC was continuously operated in a batch mode for three months.

329 The experimental data presented in Figure 4 illustrate the voltage generation of the H-

330 type MFC and the theoretical COD removal rate in the liquid bulk.

331 [FIGURE 4 NEAR HERE]

332 As seen in Figure 4, the electricity generation was proportional to the theoretical COD

333 removal rate in the system. In this figure, several sections can be identified. Initially,

334 the system presented an exponential increase of the voltage, which could be explained

335 because of the high consumption rate of the substrates by the microorganisms in the

336 anodic chamber. A maximum voltage output of 12.0 mV was observed after 15 d of the

337 start-up, which corresponds to a CE of approximately 1.5%.

338 After achieving the maximum in the voltage exerted, the voltage gradually dropped to

339 approximately 6.0 mV. Over more than 40 d, the voltage was maintained at

340 approximately 6.0 mV, with an average CE of approximately 2.5%. This result could be

341 explained because of the almost constant COD consumption rate of approximately 0.3

342 g COD (g COD d)$^{-1}$. The low CE can be explained by a very high glucose concentration

343 (9.6 g COD L^{-1}) in the anodic chamber. This finding could be related to the fact that the

344 conventional anaerobic organisms outcompete the electrogenic ones when working at

345 very high glucose concentrations. In the literature (Velasquez-Orta et al., 2011), similar

346 results were reported for studies working with high glucose concentrations. Finally,

347 after approximately 70 d of operation, the voltage decreased again to approximately

348 0.5 mV, which may be related to endogenous electricity generation.

349 *3.2.2 Substrate transformation*

16

350   Regarding the use of glucose as a fuel, it is remarked that the slight pH reduction

351   observed (from 7 to approximately 6) and the long-lasting voltage generation over

352   more than 100 d (even when the glucose was exhausted after only 20 d) indicated that

353   the glucose added to the MFC was transformed in the anodic chamber. Because of the

354   importance of the fermentation process in the MFC (Lee et al., 2008), the glucose

355   concentration and the fermentation product concentrations were monitored (see

356   Figure 5). In Figure 5, it can be seen that the MFC performed fermentation apart from

357   power generation.

358   [FIGURE 5 NEAR HERE]

359   During the first 20 d of the operation of the closed circuit MFC, the main

360   transformations can be explained because of the glucose fermentation to ethanol and

361   lactic acid, as occurred in the open circuit MFC.

362   As seen in Figure 5, the glucose was consumed in approximately 20 d. During this

363   period, several fermentation products appeared in the anodic liquid bulk, with ethanol

364   and lactic acid being the most relevant, but acetic and formic acids also appeared,

365   similar to the open circuit MFC. Considering the comparison of the production of the

366   fermentation products in the open and closed circuit MFCs, the existence of a lag

367   phase in the lactic acid production under closed circuit conditions is remarkable. To

368   account for this difference, a switch function in the lactic acid production rate (see

369   process B2 in Table 2) was included. Furthermore, a slightly higher formic acid

370   production must be noted when working under closed circuit conditions. In the closed

371   circuit, formic acid was generated at a rate of approximately 0.03 g COD (g COD d)$^{-1}$

372   and with a yield of 0.08 mol COD of formic acid per mol COD of glucose. This higher

373   production could be explained because of the higher pH in the bulk liquid when
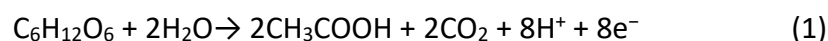
17

374 operating under closed circuit conditions. In the literature (Temudo et al., 2007), it has

375 been reported that formic acid production is favored at high pH values. The higher pH

376 values observed under closed circuit conditions could be explained by the acid

377 oxidation by electrogenic organisms and proton consumption in the cathodic

378 compartment of the MFC.

379 In principle, because the fermentation process takes place in the anodic chamber,

380 some of the electricity generation during the first 20 d of the experiment could be

381 explained because of the electrogenic fermentation of glucose (Catal et al., 2011). This

382 event could be possible in an MFC because there are different fermentation pathways

383 that could be divided into two groups, including the electricity generation processes

384 (Reactions (1-3)) and the conventional fermentation processes (Fang & Liu, 2002; Fang

385 et al., 2002). The latter processes do not generate electricity (Reactions (4-8).

386
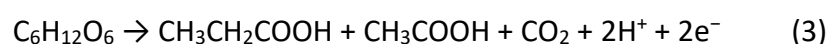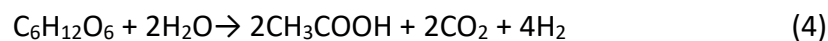
Electrogenic fermentative processes (EFP)

387
$$C_6H_{12}O_6 + 2H_2O \rightarrow 2CH_3COOH + 2CO_2 + 8H^+ + 8e^- \qquad (1)$$

388
$$C_6H_{12}O_6 \rightarrow (CH_3)_2CHCOOH + 2CO_2 + 4H^+ + 4e^- \qquad (2)$$

389
$$C_6H_{12}O_6 \rightarrow CH_3CH_2COOH + CH_3COOH + CO_2 + 2H^+ + 2e^- \qquad (3)$$

390

391

Non-electrogenic fermentative processes (NEFP)

392
$$C_6H_{12}O_6 + 2H_2O \rightarrow 2CH_3COOH + 2CO_2 + 4H_2 \qquad (4)$$

393
$$C_6H_{12}O_6 \rightarrow (CH_3)_2CHCOOH + 2CO_2 + 2H_2 \qquad (5)$$

394
$$C_6H_{12}O_6 \rightarrow CH_3CH_2COOH + CH_3COOH + CO_2 + H_2 \qquad (6)$$

395
$$C_6H_{12}O_6 \rightarrow 2C_2H_5OH + 2CO_2 \qquad (7)$$

396
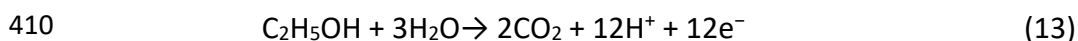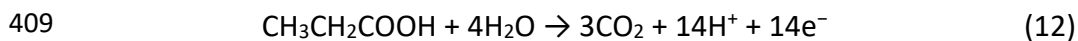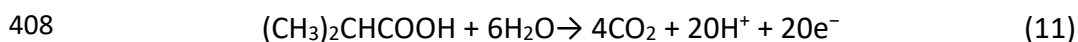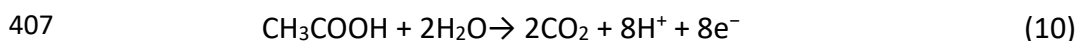$$C_6H_{12}O_6 \rightarrow 2\ CH_3CHOHCOOH \qquad (8)$$
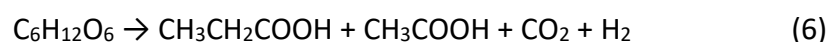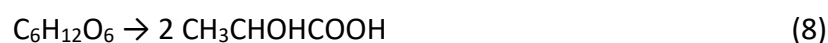
397

398 Additionally, the electricity generation in the MFC could also be due to the direct

399 conversion of glucose to CO_2 (Reaction (9)) and the conversion of the fermentation

400 products generated to CO_2 (Reactions (10-14). The sum of all of these contributions

401 could explain why the peak in the electricity generation was reached at 15 d after the

402 start-up of the MFC. After that peak, the glucose was exhausted; therefore, only the

403 fermentation products could have been used for electricity generation.

404

405 **_Electrogenic oxidative processes (EOP)_**

406 $C_6H_{12}O_6 + 12H_2O \rightarrow 6CO_2 + 24H^+ + 24e^-$ (9)

407 $CH_3COOH + 2H_2O \rightarrow 2CO_2 + 8H^+ + 8e^-$ (10)

408 $(CH_3)_2CHCOOH + 6H_2O \rightarrow 4CO_2 + 20H^+ + 20e^-$ (11)

409 $CH_3CH_2COOH + 4H_2O \rightarrow 3CO_2 + 14H^+ + 14e^-$ (12)

410 $C_2H_5OH + 3H_2O \rightarrow 2CO_2 + 12H^+ + 12e^-$ (13)

411 $CH_3CHOHCOOH + 3H_2O \rightarrow 3CO_2 + 12H^+ + 12e^-$ (14)
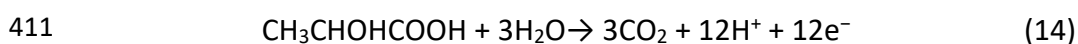
412

413 Taking the above reactions into account, the voltage produced during the first stage

414 (see Figure 4) could be related to the electrogenic fermentation of glucose, the non-

415 electrogenic glucose fermentation and the subsequent electrogenic oxidation of the

416 fermentation products, or it could be due to the electrogenic oxidation of glucose to

417 CO_2.

418 In this work, it is important to note that the main fermentation products accumulated

419 in the liquid bulk of both MFCs (open and closed circuit), corresponding to those not

420 generated by means of the electricity generation processes (reactions 7-8). There are

19

421 two possible explanations for this finding, including a negligible contribution of these

422 electricity generating processes in the closed circuit MFC or a quick consumption of the

423 fermentation products generated by means of the electrogenic fermentative

424 processes. In this work, the latter explanation was refused based on the conclusions

425 reported in the literature when fermenting monosaccharides in MFCs (Catal et al.,

426 2011).

427 During the second stage (see Figure 4), the main reaction generating electricity was

428 the oxidation of the fermentation products previously generated, particularly ethanol,

429 which was the main fermentation product consumed. In this work, lactic acid was not

430 consumed, which is in accordance with Thurston (1985), who reported the generation

431 of lactic acid in a MFC without further utilization to generate electricity under

432 anaerobic conditions (Thurston et al., 1985).

433 Finally, the third stage (see Figure 4), which is characterized by a very low voltage

434 generation, could be explained due to the oxidation of traces of SCFA presented in the

435 liquid bulk or to endogenous electricity generation. However, taking the almost

436 negligible soluble COD removal rate into account, the most probable explanation is

437 endogenous electricity generation.

438 Because of the simultaneous generation and consumption of ethanol in the closed

439 circuit MFC, it was considered interesting to uncouple the generation/consumption of

440 ethanol and determine the kinetics and stoichiometric parameters for ethanol

441 consumption in a specific experiment. Hence, an additional experiment was performed

442 in an identical H-type MFC fed with ethanol at 6.0 g COD L^{-1}. In this experiment, the

443 ethanol consumption and the electricity generation were studied, and the results are

444 presented in Figure 6.

20

445   [FIGURE 6 NEAR HERE]

446   It can be seen in Figure 6 that the system started to degrade the ethanol and produce

447   electricity after a short acclimatization period. The ethanol degradation rate was

448   almost constant over the course of the experiment. Once the electricity generation

449   started, the voltage generated increased, reaching a maximum voltage generation of

450   approximately 7 mV. This voltage generation was maintained for approximately 70 d

451   and then decreased, reaching a new steady state at approximately 1 mV. In the

452   absence of substrate, this result can only be explained by endogenous electrogenic

453   generation.

454   With the aim of determining the main kinetics and stoichiometric parameters of the

455   electrogenic ethanol oxidation, the equations describing the ethanol consumption and

456   the coupled electricity generation (see process E2 in Table 1) were fitted to the

457   experimental results, with the ethanol degradation rate being 0.3 g COD (g COD d)$^{-1}$

458   and the half-saturation coefficient being 0.96 g COD L^{-1}. The K_S value obtained is very

459   similar to that referenced in the literature (Kim et al., 2007). The equations proposed,

460   as well as the parameter values obtained, were subsequently used for fitting the

461   closed circuit experimental data obtained when glucose was used for the electricity

462   generation.

463   Once the kinetics and stoichiometric parameters of the fermentation, as well as those

464   of the ethanol oxidation and the associated electricity production, were determined,

465   all of the equations of the MFC model were used to simulate the experimental data set

466   obtained in the experiment performed with glucose in the closed circuit H-type MFC.

467   The kinetics and stoichiometric parameters obtained through the fermentation and in

468   the ethanol electrogenic oxidation tests were used in the model. The obtained results

21

469 accurately predict the evolution of the substrate, the fermentation product profiles

470 and the electricity production in the H-type MFC, as seen from the model predictions

471 and the actual data presented in Figures 5 and 6. The values of the main kinetics and

472 stoichiometric parameters obtained from the fitting are summarized in Table 4. It was

473 only necessary to include a small amount of glucose oxidation to accurately fit the

474 electricity production.

475 From the obtained results, it is interesting to note the almost negligible oxidation rate

476 of glucose by anodophilic organisms: 0.03 g COD (g COD d)$^{-1}$. A possible explanation is

477 that the direct anodic oxidation of glucose by pure electrogenic cultures, which has

478 been previously observed (Chaudhuri & Lovley, 2003), may not be the most important

479 pathway when working with mixed cultures (Freguia et al., 2008). This phenomenon

480 could be due to the very low concentration of electrogenic microorganisms in the

481 mixed culture. Another possible explanation is the lower affinity and lower maximum

482 consumption rate of the substrate by the electrogenic microorganisms compared with

483 the conventional ones. This notion was confirmed when comparing the carbon

484 consumption rate in the fermentation process with the electrogenic ethanol and

485 glucose oxidation. The carbon consumption rate during the glucose fermentation

486 process was approximately 16 mmol C (L d)$^{-1}$, whereas the carbon consumption rate

487 during the electrogenic ethanol and glucose consumption was ten times lower

488 (approximately 1.5 mmol C (L d)$^{-1}$).

489 The biomass growth in the system was fitted using an endogenous decay rate of 0.02

490 d^{-1} and a biomass yield of 0.07 g COD (g COD)$^{-1}$ (Romli et al., 1995). According to

491 theoretical values, the oxidative aerobic biomass growth accounted for approximately

492 40% of the carbon consumption, and the anaerobic one accounted for approximately

493   5%. The value proposed in this work corresponds to a weighted value between both

494   processes, i.e., the anaerobic one (fermentative) and the oxidative one (electrogenic).

495   Similar values for the biomass growth in MFCs have been observed in previous studies

496   (Kim et al., 2011).

497   In the closed systems fed with glucose or ethanol, the electrons transported through

498   the circuit represented a small portion, ranging from 1 to 3%. This finding could be

499   explained by the loss of MFC electrons by overpotential, ohmic resistance and the

500   inefficient oxidation of fermentation products and glucose.

501   [TABLE 4 NEAR HERE]

502

503   *3.3 Model validation*

504   Once the calibration procedure was finished, the developed model was compared and

505   validated using data from a new experiment. During the validation, a satisfactory

506   agreement was obtained between the measured and predicted values. The goodness

507   of fit was determined by the Mean Relative Squared Error (MRSE) criterion. The MRSE

508   values obtained during the calibration and validation stages are presented in Table 5.

509   The obtained results show that the model accuracy was maintained during the

510   validation stage, with a MRSE value of 12.3%, a value very similar to that obtained

511   during the calibration of the model.

512   [TABLE 5 NEAR HERE]

513

514 **CONCLUSIONS**

515

516 In this work, a model describing the evolution of a MFC fed with high glucose

517 concentrations was developed. Comparing open and closed circuit operation of the

518 MFC, similar reaction extensions and product distributions of the fermentation process

519 were observed. From the obtained results, the importance of the fermentation process

520 in electricity production was shown by the high ethanol consumption rate by

521 electrogenic organisms (0.3 g COD (g COD d)$^{-1}$) compared with that of the glucose (0.03

522 g COD (g COD d)$^{-1}$). In terms of electricity generation, ethanol contributed to

523 approximately 90% the production, whereas glucose accounted for only 10% of the

524 production.

525

526 **Acknowledgements**

529

530

531

24

References

Brillas, E., Martínez-Huitle, C.A. 2015. Decontamination of wastewaters containing synthetic organic dyes by electrochemical methods. An updated review. *Applied Catalysis B: Environmental*, **166-167**, 603-643.

Catal, T., Fan, Y., Li, K., Bermek, H., Liu, H. 2011. Utilization of mixed monosaccharides for power generation in microbial fuel cells. *Journal of Chemical Technology and Biotechnology*, **86**(4), 570-574.

Chandrappa, R., Das, D.B. 2014. *Sustainable Water Engineering : Theory and Practice*. Wiley, Chichester.

Chaudhuri, S.K., Lovley, D.R. 2003. Electricity generation by direct oxidation of glucose in mediatorless microbial fuel cells. *Nature Biotechnology*, **21**(10), 1229-1232.

De Lucas, A., Rodriguez, L., Villasenor, J., Fernandez, F.J. 2005. Denitrification potential of industrial wastewaters. *Water Research*, **39**(15), 3715-3726.

de Lucas, A., Rodríguez, L., Villaseñor, J., Fernández, F.J. 2007. Fermentation of agro-food wastewaters by activated sludge. *Water Research*, **41**(8), 1635-1644.

Eaton, A.D., Clesceri, L.S., Rice, E.W., Greenberg, A.E., Franson, M.A.H., American Public Health Association., American Water Works Association., Water Environment Federation., APHA., AWWA., WEF. 2005. *Standard methods for the examination of water and wastewater*. *21st ed*. American Public Health Association, Washington.

Edwards, V.H. 1970. The influence of high substrate concentrations on microbial kinetics. *Biotechnology and Bioengineering*, **12**(5), 679-712.

Fang, H.H.P., Liu, H. 2002. Effect of pH on hydrogen production from glucose by a mixed culture. *Bioresource Technology*, **82**(1), 87-93.

Fang, H.H.P., Liu, H., Zhang, T. 2002. Characterization of a hydrogen-producing granular sludge. *Biotechnology and Bioengineering*, **78**(1), 44-52.

Fernández, F.J., Castro, M.C., Rodrigo, M.A., Cañizares, P. 2011a. Reduction of aeration costs by tuning a multi-set point on/off controller: A case study. *Control Engineering Practice*, **19**(10), 1231-1237.

Fernández, F.J., Villaseñor, J., Infantes, D. 2011b. Kinetic and stoichiometric modelling of acidogenic fermentation of glucose and fructose. *Biomass and Bioenergy*, **35**(9), 3877-3883.

Fernández-Morales, F.J., Villaseñor, J., Infantes, D. 2010. Modeling and monitoring of the acclimatization of conventional activated sludge to a biohydrogen producing culture by biokinetic control. *International Journal of Hydrogen Energy*, **35**(20), 10927-10933.

Freguia, S., Rabaey, K., Yuan, Z., Keller, J. 2008. Syntrophic processes drive the conversion of glucose in microbial fuel cell anodes. *Environmental Science and Technology*, **42**(21), 7937-7943.

Gonzalez del Campo, A., Lobato, J., Cañizares, P., Rodrigo, M.A., Fernandez Morales, F.J. 2013. Short-term effects of temperature and COD in a microbial fuel cell. *Applied Energy*, **101**, 213-217.

Infantes, D., González Del Campo, A., Villaseñor, J., Fernández, F.J. 2011. Influence of pH, temperature and volatile fatty acids on hydrogen production by acidogenic fermentation. *International Journal of Hydrogen Energy*, **36**(24), 15595-15601.

Karimi Alavijeh, M., Mardanpour, M.M., Yaghmaei, S. 2015. A generalized model for complex wastewater treatment with simultaneous bioenergy production using the microbial electrochemical cell. *Electrochimica Acta*, **167**, 84-96.

Kim, J.R., Jung, S.H., Regan, J.M., Logan, B.E. 2007. Electricity generation and microbial community analysis of alcohol powered microbial fuel cells. *Bioresource Technology*, **98**(13), 2568-2577.

Kim, K.Y., Chae, K.J., Choi, M.J., Ajayi, F.F., Jang, A., Kim, C.W., Kim, I.S. 2011. Enhanced Coulombic efficiency in glucose-fed microbial fuel cells by reducing metabolite electron losses using dual-anode electrodes. *Bioresource Technology*, **102**(5), 4144-4149.

Lee, H.S., Parameswaran, P., Kato-Marcus, A., Torres, C.I., Rittmann, B.E. 2008. Evaluation of energy-conversion efficiencies in microbial fuel cells (MFCs) utilizing fermentable and non-fermentable substrates. *Water Research*, **42**(6-7), 1501-1510.

Logan, B.E., Hamelers, B., Rozendal, R., Schröder, U., Keller, J., Freguia, S., Aelterman, P., Verstraete, W., Rabaey, K. 2006. Microbial fuel cells: Methodology and technology. *Environmental Science and Technology*, **40**(17), 5181-5192.

MacKie, D.M., Liu, S., Benyamin, M., Ganguli, R., Sumner, J.J. 2013. Direct utilization of fermentation products in an alcohol fuel cell. *Journal of Power Sources*, **232**, 34-41.

Monod, J. 1949. THE GROWTH OF BACTERIAL CULTURES. *Annual Review of Microbiology*, **3**, 371-394.

Ortiz-Martínez, V.M., Salar-García, M.J., de los Ríos, A.P., Hernández-Fernández, F.J., Egea, J.A., Lozano, L.J. 2015. Developments in microbial fuel cell modeling. *Chemical Engineering Journal*, **271**, 50-60.

Picioreanu, C., Katuri, K.P., Head, I.M., Van Loosdrecht, M.C.M., Scott, K. 2008. Mathematical model for microbial fuel cells with anodic biofilms and anaerobic digestion. in: *Water Science and Technology*, Vol. 57, pp. 965-971.

Picioreanu, C., Katuri, K.P., Van Loosdrecht, M.C.M., Head, I.M., Scott, K. 2010a. Modelling microbial fuel cells with suspended cells and added electron transfer mediator. *Journal of Applied Electrochemistry*, **40**(1), 151-162.

Picioreanu, C., van Loosdrecht, M.C.M., Curtis, T.P., Scott, K. 2010b. Model based evaluation of the effect of pH and electrode geometry on microbial fuel cell performance. *Bioelectrochemistry*, **78**(1), 8-24.

Premier, G.C., Kim, J.R., Massanet-Nicolau, J., Kyazze, G., Esteves, S.R.R., Penumathsa, B.K.V., Rodríguez, J., Maddy, J., Dinsdale, R.M., Guwy, A.J. 2013. Integration of biohydrogen, biomethane and bioelectrochemical systems. *Renewable Energy*, **49**, 188-192.

Rao, J.R., Richter, G.J., Von Sturm, F., Weidlich, E. 1976. The performance of glucose electrodes and the characteristics of different biofuel cell constructions. *Bioelectrochemistry and Bioenergetics*, **3**(1), 139-150.

Rodríguez, L., Villaseñor, J., Fernández, F.J. 2007. Use of agro-food wastewaters for the optimisation of the denitrification process. in: *Water Science and Technology*, Vol. 55, pp. 63-70.

Romli, M., Keller, J., Lee, P.L., Greenfield, P.F. 1995. Model prediction and verification of a two-stage high-rate anaerobic wastewater treatment system subjected to shock loads. *Process Safety and Environmental Protection: Transactions of the Institution of Chemical Engineers, Part B*, **73**(2), 151-154.

Schröder, U. 2007. Anodic electron transfer mechanisms in microbial fuel cells and their energy efficiency. *Physical Chemistry Chemical Physics*, **9**(21), 2619-2629.

Temudo, M.F., Kleerebezem, R., Van Loosdrecht, M. 2007. Influence of the pH on (Open) mixed culture fermentation of glucose: A chemostat study. *Biotechnology and Bioengineering*, **98**(1), 69-79.

Thurston, C.F., Bennetto, H.P., Delaney, G.M. 1985. Glucose metabolism in a microbial fuel cell. Stoichiometry of product formation in a thionine-mediated Proteus vulgaris fuel cell and its relation to coulombic yields. *Journal of General Microbiology*, **131**(6), 1393-1401.

Velasquez-Orta, S.B., Yu, E., Katuri, K.P., Head, I.M., Curtis, T.P., Scott, K. 2011. Evaluation of hydrolysis and fermentation rates in microbial fuel cells. *Applied Microbiology and Biotechnology*, **90**(2), 789-798.

632

Table 1. Petersen matrix, containing the main processes taking place in the microbial fuel cell.

Table 2. Parameters used in the MFC model.

Table 3. Comparison of carbon and electron balances amongst glucose feed (open and closed circuits) after completion of anodic reactions.

Table 4. Main parameter values obtained from the model fitting to the MFC performance.

Table 5. Calibration and validation MRSE values.

Process \\ Components	1 Glucose	2 Ethanol	3 Lactic	4 Acetic	5 Butyric	6 Formic	7 H$_2$	8 IC	9 Electricity	10 Process rate
Biological conversion										
(B1) Ethanol production	-1	$(1-Y_b)f_{e,g}$						$-\sum C_i v_{i,B1}$		$k_{G,E}\dfrac{S_G}{K_{S_G}+S_G}X$
(B2) Lactic production	-1		$(1-Y_b)f_{l,g}$							$k_{G,L}\dfrac{S_G}{K_{S_G}+S_G}X\left[exp\left(\dfrac{K_G-S_G}{K_{S_G}}I_X\right)\right]$
(B3) Acetic production	-1			$(1-Y_b)f_{a,g}$			$(1-Y_b)f_{H2a,g}$	$-\sum C_i v_{i,B3}$		$k_{G,Ac}\dfrac{S_G}{K_{S_G}+S_G}X$
(B4) Butyric production	-1				$(1-Y_b)f_{b,g}$		$(1-Y_b)f_{H2b,g}$	$-\sum C_i v_{i,B4}$		$k_{G,B}\dfrac{S_G}{K_{S_G}+S_G}X$
(B5) Formic production						$(1-Y_b)f_{j,IC}$	-1	$-\sum C_i v_{i,B5}$		$K_{IC,E}\dfrac{S_{IC}}{K_{S_{IC}}+S_{IC}}X$
Electrochemical conversion										
(E1) Electrogenic glucose oxidation	-1							$-\sum C_i v_{i,E1}$	$(1-Y_b)\gamma_{e^-,COD}$	$k_{G,e^-}\dfrac{S_G}{K_{S_G}+S_G}\dfrac{S_{Mox}}{K_{Mox}+S_{Mox}}X$
(E2) Electrogenic ethanol oxidation		-1						$-\sum C_i v_{i,E2}$	$(1-Y_b)\gamma_{e^-,COD}$	$k_{E,e^-}\dfrac{S_E}{K_{S_E}+S_E}\dfrac{S_{Mox}}{K_{Mox}+S_{Mox}}X$

Parameter	Description	Unit
Biological Conversion		
S_G	Glucose concentration	g COD · L^{-1}
S_E	Ethanol concentration	g COD · L^{-1}
S_{Mox}	Oxidised mediator concentration	g COD · L^{-1}
X	Biomass concentration	g COD · L^{-1}
Y_b	Biomass yield coefficient	g COD Biomass · (g COD glucose)$^{-1}$
$f_{product,substrate}$	Catabolic yield of product on substrate	g COD product · (g COD substrate)$^{-1}$
$k_{G,E}$	Glucose to Ethanol fermentation rate	g COD Glucose · (g COD biomass·d)$^{-1}$
$k_{G,L}$	Glucose to Lactic acid fermentation rate	g COD Glucose · (g COD biomass·d)$^{-1}$
$k_{G,Ac}$	Glucose to Acetic acid fermentation rate	g COD Glucose · (g COD biomass·d)$^{-1}$
$k_{G,B}$	Glucose to Butyric acid fermentation rate	g COD Glucose · (g COD biomass·d)$^{-1}$
K_{S_G}	Monod half-saturation coefficient for glucose	g COD Glucose · L^{-1}
K_{S_E}	Monod half-saturation coefficient for ethanol	g COD Ethanol · L^{-1}
K_{Mox}	Monod half-saturation coefficient for oxidised mediator	g COD Oxidised mediator · L^{-1}
K_G	Glucose switching constant	g COD Glucose · L^{-1}
C_i	Carbon content of component i	mole C · g COD^{-1}
v_i	Rate coefficient for component I on process j	g COD · m^{-3}
I_X	Open-closed circuit Boolean switching function	
Electrochemical Conversion		
k_{G,e^-}	Electrogenic Glucose oxidation rate	g COD Glucose · (g COD biomass·d)$^{-1}$
k_{E,e^-}	Electrogenic Ethanol oxidation rate	g COD Ethanol · (g COD biomass·d)$^{-1}$
$\gamma_{COD}^{e^-}$	Electricity generation from COD oxidation	12060 Coulombs · g COD^{-1}

	Glucose open circuit		Glucose closed circuit	
	Carbon Balance		**Carbon Balance**	
	C mmol	**Fraction %**	**C mmol**	**Fraction %**
Amount Added				
Glucose	268.09	100.00	257.25	100.00
Final recovery				
Ethanol	95.20	35.51	0.00	0.00
Lactic acid	69.30	25.85	69.51	27.02
Formic acid	1.40	0.52	4.20	1.63
Acetic acid	0.35	0.13	0.56	0.22
Butyric acid	0.00	0.00	0.03	0.01
Carbon dioxide	45.85	17.10	139.37	54.18
Biomass growth	20.20	7.53	18.34	7.13
Total recovery	*232.30*	*86.65*	*232.01*	*90.19*

Parameter	Value	Parameter	Value	Parameter	Value
		Biological Conversion		Electrochemical Conversion	
Y_b	0.07 g COD · (g COD)$^{-1}$	$f_{H2b,g}$	0.17 g COD · (g COD)$^{-1}$	k_{m,Ee^-}	0.3 g COD · (g COD·d)$^{-1}$
$f_{e,g}$	0.88 g COD · (g COD)$^{-1}$	$k_{G,E}$	2.67 g COD · (g COD·d)$^{-1}$	k_{m,Ge^-}	0.03 g COD · (g COD·d)$^{-1}$
$f_{l,g}$	0.68 g COD · (g COD)$^{-1}$	$k_{G,L}$	1.72 g COD · (g COD·d)$^{-1}$		
$f_{a,g}$	0.50 g COD · (g COD)$^{-1}$	K_{S_G}	1.9 g COD Glucose · l^{-1}		
$f_{H2a,g}$	0.50 g COD · (g COD)$^{-1}$	K_{S_E}	1.0 g COD Ethanol · l^{-1}		
$f_{b,g}$	0.83 g COD · (g COD)$^{-1}$	K_G	5.8 g COD Glucose · l^{-1}		

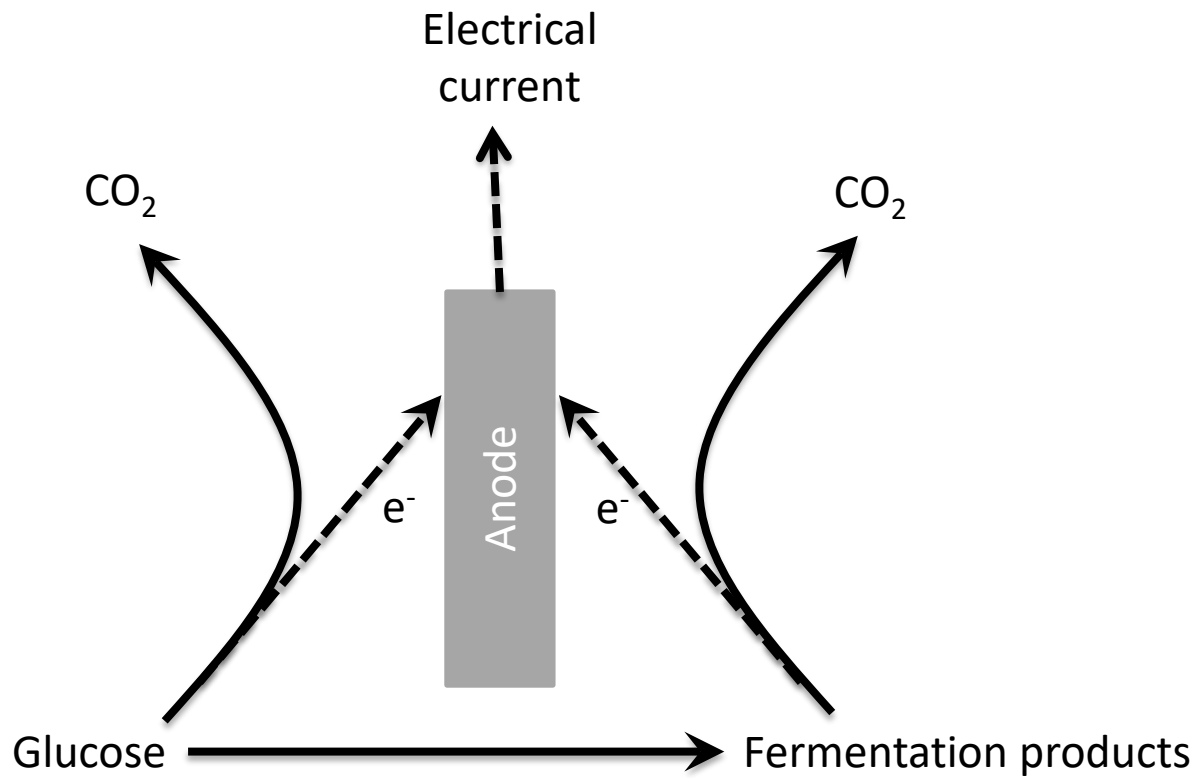|	Open circuit MFC	Ethanol MFC	Closed circuit MFC
Calibration data	15.1	21.5	10.5
Validation data			12.3

Figure 1. A concept of the bio-electro-chemical model based on the glucose fermentation, supplemented with the glucose and ethanol oxidation with electron-transfer to the electrode.
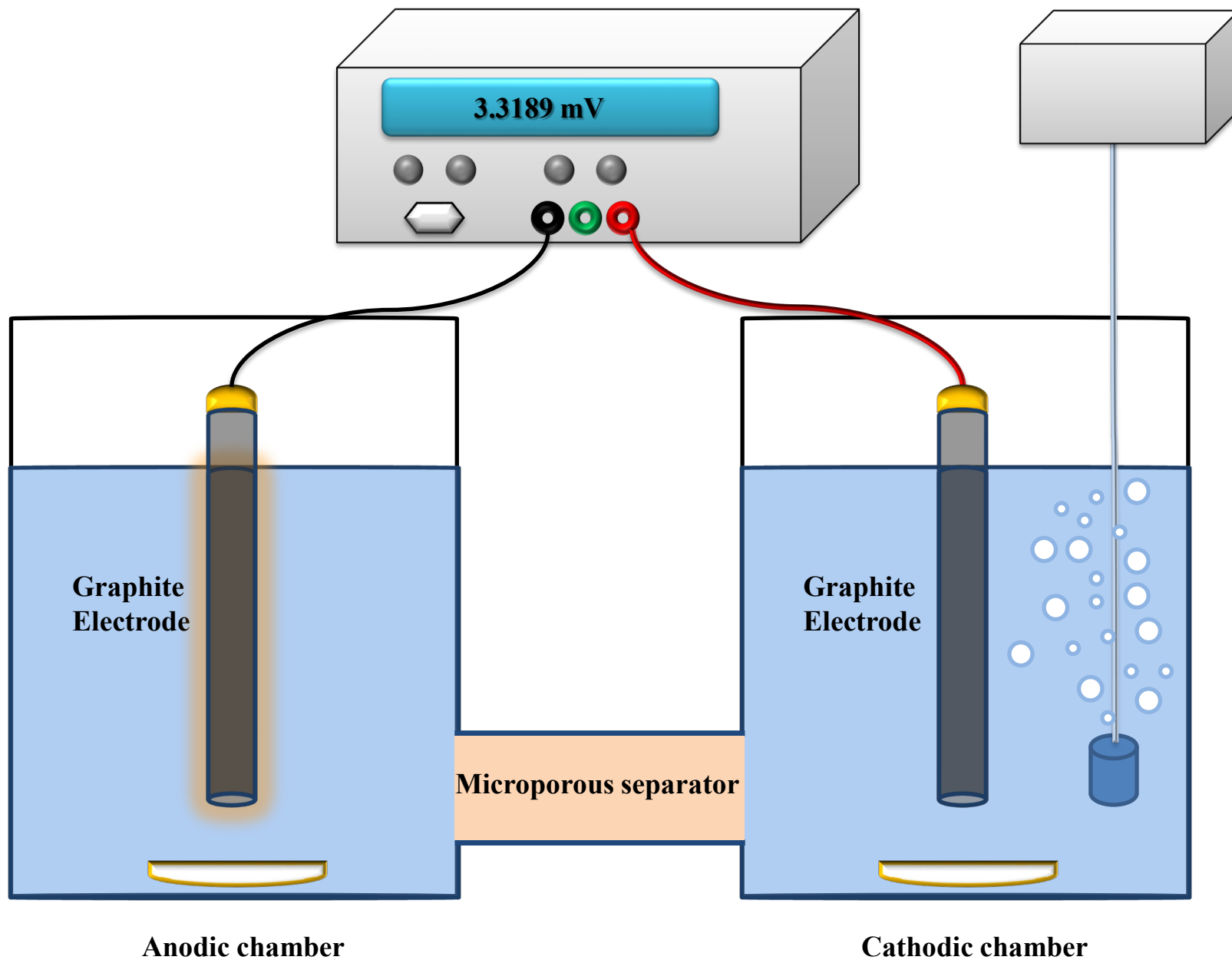
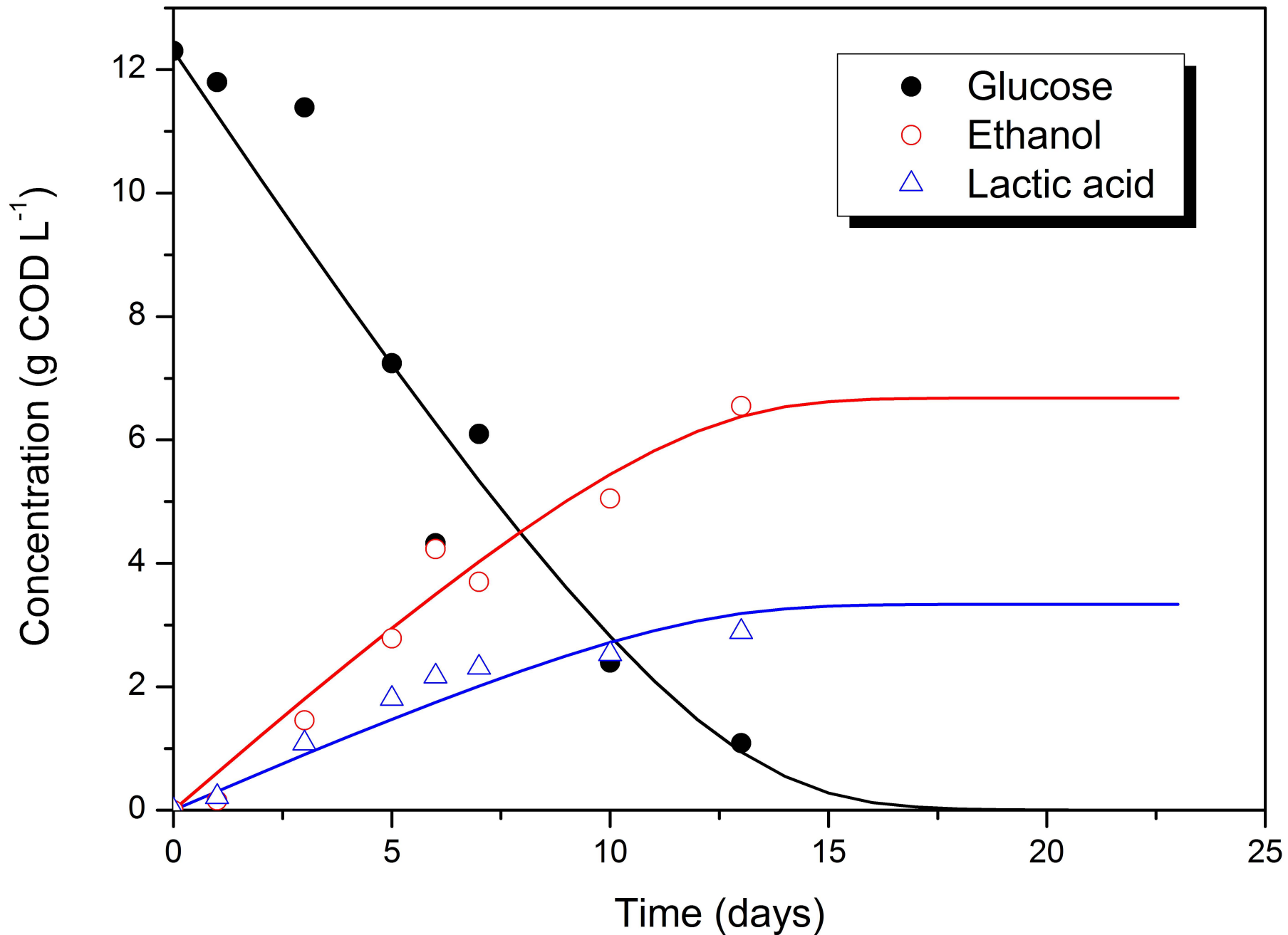Figure 2. Schematic view of the H-type MFC set-up.

Figure 3. Performance of the H-type MFC under open circuit conditions (Solid lines correspond to model predictions).

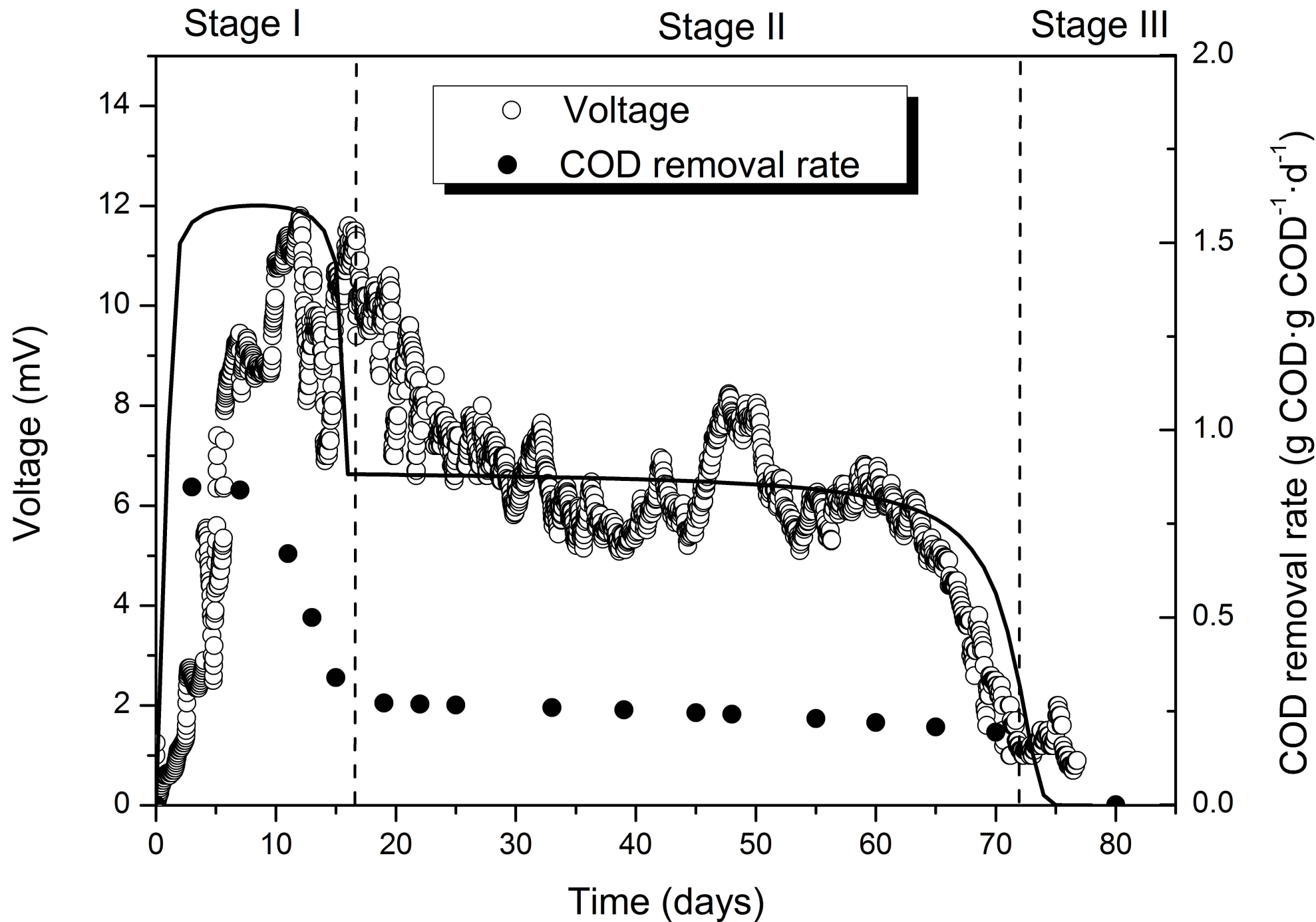Figure 4. Voltage generation and theoretical COD consumption rate in the H-type MFC fed with glucose (Solid lines correspond to voltage prediction).

Figure 5. Substrate and main products profiles during the closed circuit experiment (Solid lines correspond to model predictions).

Figure 6. Electricity generation and ethanol concentration profile in the MFC feed with ethanol (Solid lines correspond to model predictions).

Figure 1. A concept of the bio-electro-chemical model based on the glucose fermentation, supplemented with the glucose and ethanol oxidation with electron-transfer to the electrode.

Figure 2. Schematic view of the H-type MFC set-up.

Multimeter

3.3189 mV

Aquarium air pump

Graphite Electrode

Graphite Electrode

Microporous separator

Anodic chamber

Cathodic chamber

Figure 3. Performance of the H-type MFC under open circuit conditions (Solid lines correspond to model predictions).

Figure 4. Voltage generation and theoretical COD consumption rate in the H-type MFC fed with glucose (Solid lines correspond to voltage prediction).
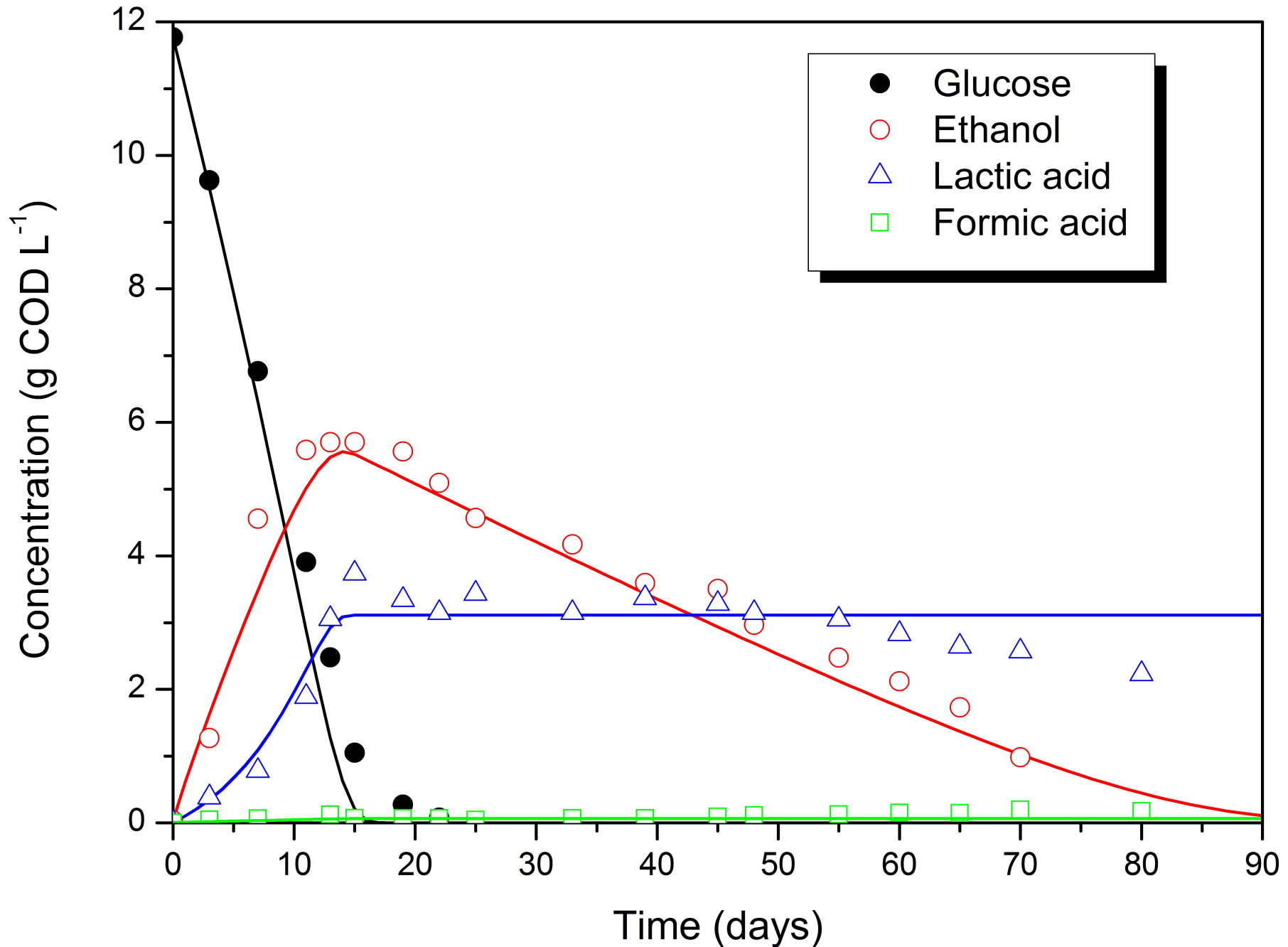
Figure 5. Substrate and main products profiles during the closed circuit experiment (Solid lines correspond to model predictions).